

Positive pion photoproduction from ^{10}B and ^{16}O

V. DeCarlo* and N. Freed

Department of Physics, The Pennsylvania State University, University Park, Pennsylvania 16802

(Received 8 December 1981)

Differential and total cross sections for the reactions $^{10}\text{B}(\gamma, \pi^+)^{10}\text{Be}$ and $^{16}\text{O}(\gamma, \pi^+)^{16}\text{N}$ are calculated within the distorted wave impulse approximation and compared to experiment and to the results of similar calculations with different versions of the elementary photoproduction amplitudes, nuclear wave functions, and π -nucleus optical potentials. Although the calculated results are in fairly good agreement with each other, discrepancies with experiment are much in evidence.

[NUCLEAR REACTIONS $^{10}\text{B}(\gamma, \pi^+)^{10}\text{Be}$, $^{16}\text{O}(\gamma, \pi^+)^{16}\text{N}$. Calculated
 $d\sigma/d\Omega$, σ ; compared with experiment, other calculations.]

It has long been recognized that pion photoproduction from nuclear systems can provide a sensitive probe of the π -nucleus interaction. To the extent that the single nucleon production amplitudes yield accurate fits to the $\gamma N \rightarrow \pi N$ process and to the degree that the nuclear wave functions are consistent with such properties as transverse electron scattering, nuclear pion photoproduction can provide a reliable test of the various π -nucleus optical potentials used to simulate final state effects over a wide range of energy and momentum transfer. This range includes the region between threshold and $T_\pi \sim 30$ MeV in which pion decay renders π -nucleus scattering data highly uncertain.

With this in mind, we have carried out calculations on the reactions $^{10}\text{B}(\gamma, \pi^+)^{10}\text{Be}$ and $^{16}\text{O}(\gamma, \pi^+)^{16}\text{N}$ from the near-threshold region to the high-energy tail of the Δ resonance and compared the results to experiment¹⁻⁵ and to several other calculations⁶⁻⁸ with different input assumptions. The recent availability of stable high-intensity electron beams and pion spectrometers has yielded accurate experimental data which, together with nuclear structure information that is consistent with electron form factors, make these calculations appropriate at this time. Our results will be compared to the distorted wave impulse approximation (DWIA) calculations of Singham and Tabakin⁶ (ST) for transitions to the ground state of ^{10}Be ; to the DWIA calculations of Nagl and Überall⁷ (NU) for transitions to the ground and first excited states in ^{10}Be and to the bound states in ^{16}N ; and to the DWIA calculations of Devanathan, Giriya, and Prasad⁸ (DGP) for transitions to the ^{16}N bound

states. ST employ the Blomqvist-Laget⁹ (BL) reduction of the elementary amplitudes together with Cohen-Kurath (CK) wave functions¹⁰ and the pion optical potential of Stricker *et al.*¹¹ (SMC). NU use the Berends *et al.* amplitudes (BDW),¹² Helm model wave functions, and a second-order optical potential of the same form as SMC but with somewhat different parameters. DGP use the Chew *et al.* amplitudes (CGLN) (Ref. 13) with pion gradient terms omitted, wave functions of Rho,¹⁴ and an optical potential of the same type as SMC but with isovector and absorption contributions ignored. The present calculations, also within the DWIA, are carried out using methods described in detail earlier.¹⁵ The elementary amplitudes are those of BDW. Since this parametrization as well as BL and CGLN provide reasonably accurate fits to single nucleon photoproduction, we expect that significant differences among calculations or between experiment and calculations should not arise from the elementary amplitudes. For $A=10$ we use the CK wave functions. These wave functions yield good fits to energy levels, β -decay rates, and $M1$ transitions throughout the p shell and, in particular, are in excellent agreement with recent Saskatchewan data¹⁶ on inelastic electron scattering to the 1.74 MeV (0^+) and 5.17 MeV (2^+) levels in ^{10}B , analogs of the ground and first excited states (3.37 MeV) in ^{10}Be . The Helm model calculations use as input the transverse (e, e') form factors which contain spin magnetization, convection current, and meson-exchange components. For $A=10$, the pure or dominant $M3$ transitions between the ground or first excited state in ^{10}Be and the ^{10}B ground state

insure that the convection contributions are quite small (identically zero for pure p -shell states).¹⁷ Near threshold, the photoproduction cross sections arise predominantly from the same spin current ($\vec{\sigma}\cdot\vec{\epsilon}$) appearing in the magnetic transition operator, thereby imparting a high degree of reliability to the Helm model predictions. At higher energies, the increasingly strong dependence of the cross sections upon the pion momentum dependent terms in the amplitude imply more uncertainty in the Helm model results. For $A=16$ we have used the wave functions of Donnelly and co-workers.¹⁸ They showed that by admixing single particle-hole states of the type $|(p)^{-1}(sd)^1\rangle$ via a realistic interaction, they could obtain an accurate description of the $T=1$ particle-hole states excited by electron scattering on ^{16}O for such properties as electron scattering form factors and muon capture and β -decay rates. The effect of including more complicated configurations was simulated by overall reduction factors which varied from cluster to cluster of near-lying configuration-mixed levels. The cluster which is

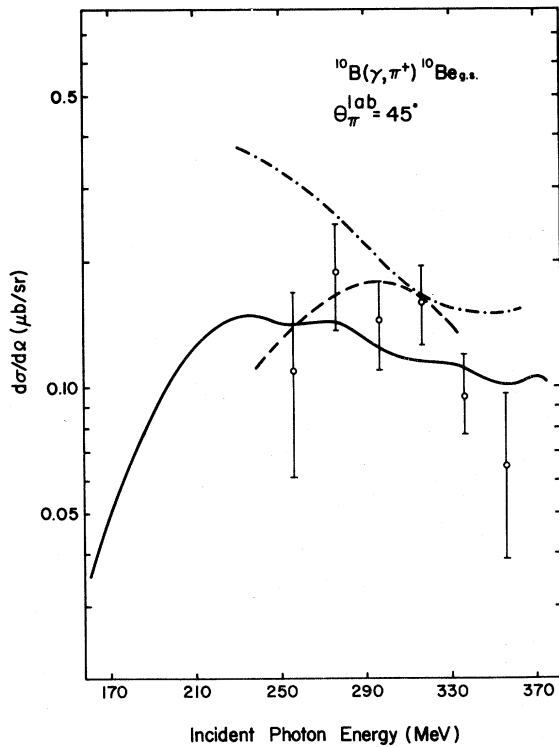


FIG. 1. Differential cross sections for $^{10}\text{B}(\gamma, \pi^+)^{10}\text{Be}_{\text{g.s.}}$ at $\theta_{\pi}^{\text{lab}} = 45^\circ$. The solid curve is the present result, the dashed curve is the result of Singham and Tabakin (Ref. 6), and the dotted-dashed curve is the result of Nagl and Überall (Ref. 7). See text for description of calculations. The data are from Bosted *et al.* (Refs. 3 and 4).

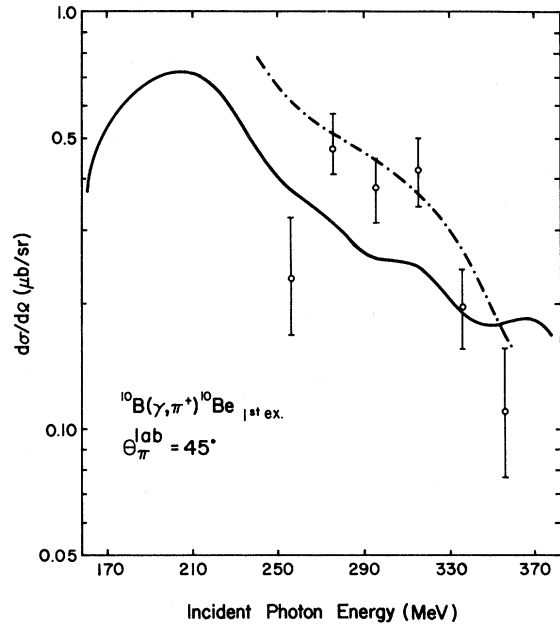


FIG. 2. Differential cross sections for $^{10}\text{B}(\gamma, \pi^+)^{10}\text{Be}_{1\text{st ex.}}$ at $\theta_{\pi}^{\text{lab}} = 45^\circ$. See caption to Fig. 1.

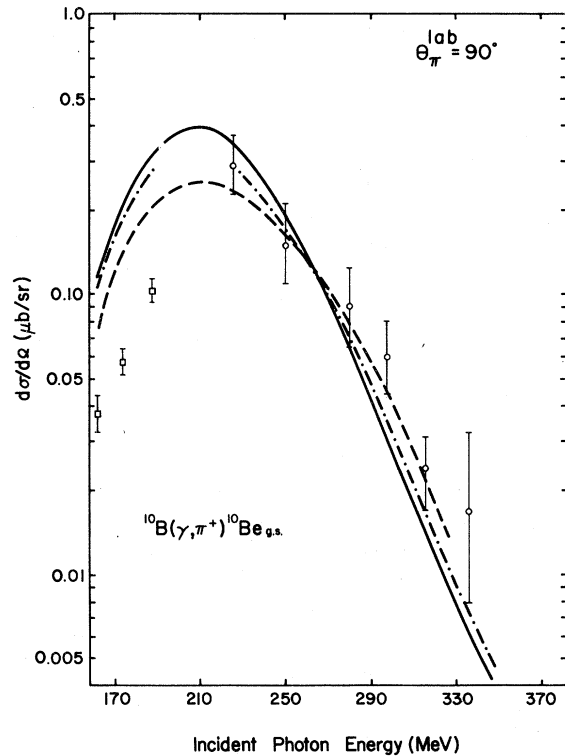


FIG. 3. Same as Fig. 1 for $\theta_{\pi}^{\text{lab}} = 90^\circ$. The low energy data points are from Rowley *et al.* (Refs. 1 and 2).

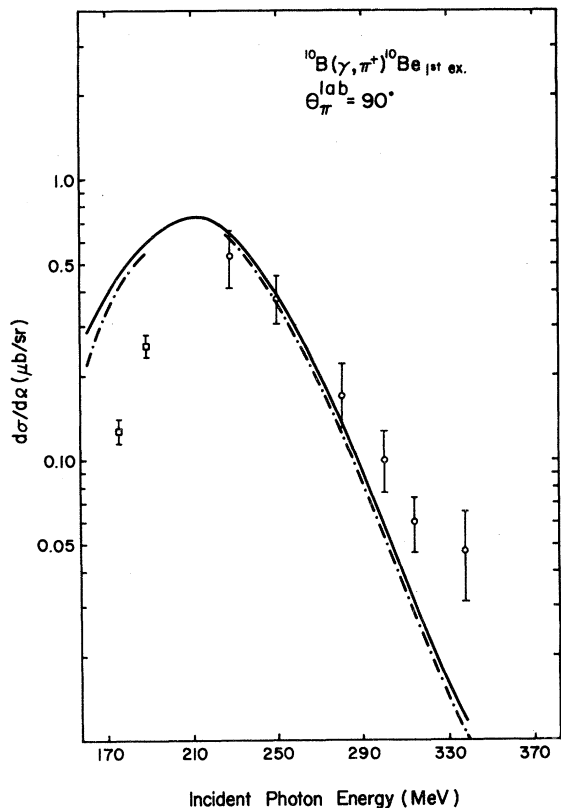


FIG. 4. Same as Fig. 2 for $\theta_{\pi}^{\text{lab}}=90^{\circ}$. See captions to Figs. 1 and 3.

analogous to the particle-stable states in ^{16}N forms a complex around 13 MeV excitation energy in ^{16}O and required a reduction factor¹⁹ in (amplitude)² of 3. The Rho wave functions used by DGP have not to our knowledge been tested on electron scattering data but are consistent with muon capture rates. Finally, we have used the SMC potential, which gives reasonably good fits to pionic atom and low-energy π -nucleus scattering data. Gaussian matter and charge distributions have been employed with parameters taken from Ref. 20. Parameter set 1 was used for low-energy ($T_{\pi} \leq 50$ MeV) scattering, with a linear interpolation made between the 50 MeV and higher energy parameters provided. We repeated our calculations for a set of redetermined 30, 40, and 50 MeV parameters²¹ and found little difference in our results; our figures use the earlier parameters. Although both NU and DGP use somewhat altered SMC potentials, it is unlikely that the modifications would yield qualitative differences in the present cross sections.

Our results are shown in Figs. 1–9. In Figs. 1

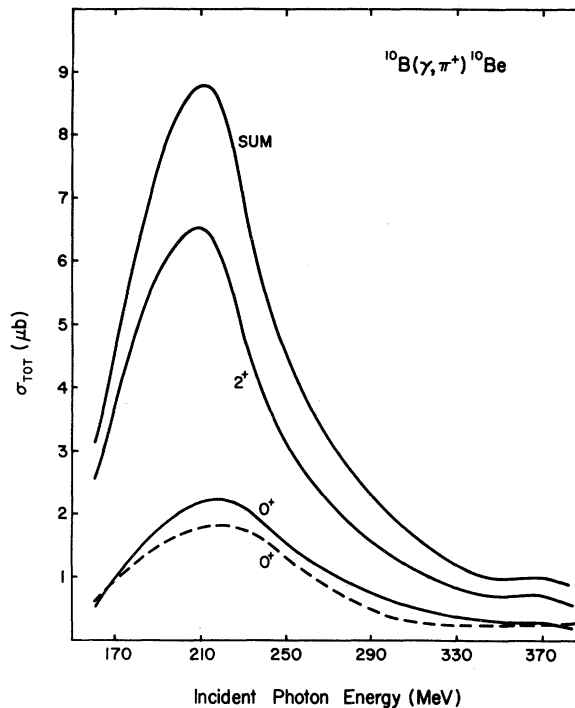


FIG. 5. Total cross sections for $^{10}\text{B}(\gamma, \pi^+)^{10}\text{Be}$ to 0^+ ground state, 2^+ first excited state, and the sum. The dashed curve uses the local Laplacian potential (Ref. 23).

and 2, we have plotted $\theta_{\pi}^{\text{lab}}=45^{\circ}$ differential cross sections for $^{10}\text{B}(\gamma, \pi^+)$ to the ground and first excited state of ^{10}Be , respectively. In Figs. 3 and 4, $\theta_{\pi}^{\text{lab}}=90^{\circ}$. Figure 5 is a plot of total cross sections to the ground and first excited states together with their sum. Experimental points and results of other calculations are as indicated. Inspection of the figures indicates that the various theoretical approaches yield results much more in agreement with each other than with experiment. This is particularly evident for 90° scattering at low energy where all theoretical results overshoot experiment by factors of 2–3 for both ground and excited state transitions. At 45° the heightened sensitivity to certain kinematic factors which are treated somewhat differently in the various theoretical approaches contributes to the discrepancies found among the results. We have not plotted the results of a recent calculation²² on this reaction which uses the CGLN amplitudes, CK wave functions, and the (first-order) local Laplacian optical potential.²³ Although the results are in good agreement with experiment, we were unable to duplicate them with any reasonable choice of local Laplacian parameters, finding

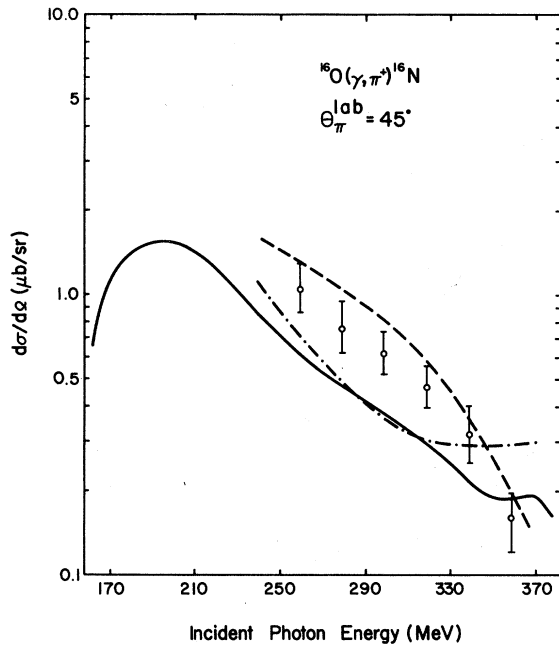


FIG. 6. Differential cross sections for $^{16}\text{O}(\gamma, \pi^+)^{16}\text{N}$ at $\theta_{\pi}^{\text{lab}}=45^\circ$ summed over all four particle-stable states in ^{16}N . The solid curve is the present result, the dashed curve is the result of Devanathan *et al.* (Ref. 8), and the dotted-dashed curve is the result of Nagl and Überall (Ref. 7). Data points are from Bosted *et al.* (Refs. 3 and 4). See text for description of calculations.

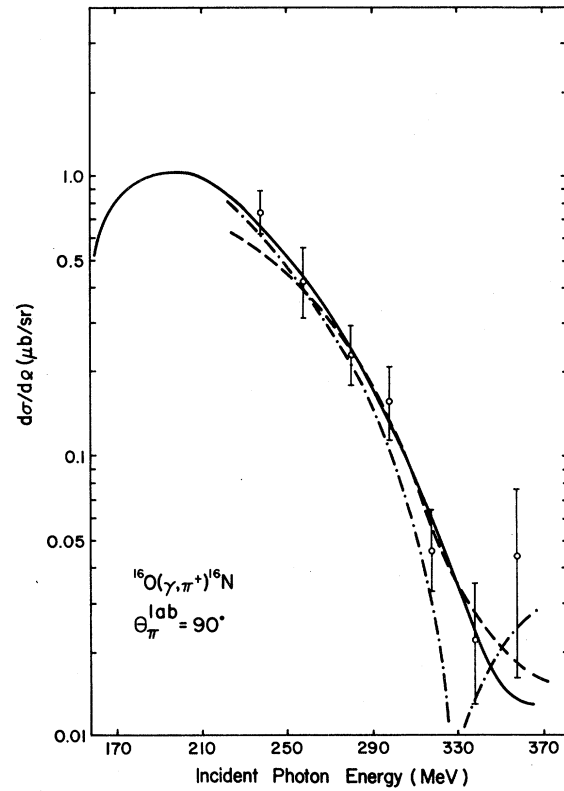


FIG. 7. Same as Fig. 6 for $\theta_{\pi}^{\text{lab}}=90^\circ$.

instead that reductions in the SMC differential or total cross sections by no more than 20% stem from use of this potential (cf., e.g., Fig. 5); this observation is consistent with the results of our recent calculation²⁴ on $^{14}\text{N}(\gamma, \pi^-)^{14}\text{O}$, where the effects of using different optical potentials were looked at in detail. Figures 6–9 are plots of our results for $^{16}\text{O}(\gamma, \pi^+)^{16}\text{N}$. In Figs. 6 and 7, $\theta_{\pi}^{\text{lab}}=45^\circ$ and $\theta_{\pi}^{\text{lab}}=90^\circ$ differential cross sections to the sum of the four ^{16}N bound states are compared to experiment and to the results of other calculations. In Fig. 8, total cross sections to each bound state are shown separately, while Fig. 9 compares the sum to the results of other calculations and to experiment. Again, the various theoretical approaches yield results that are quite similar and, for the differential cross sections, are in fairly good agreement with experiment. All three calculations are in severe disagreement with the (now 15 year old) measurements of Meyer *et al.*,⁵ which involve making large

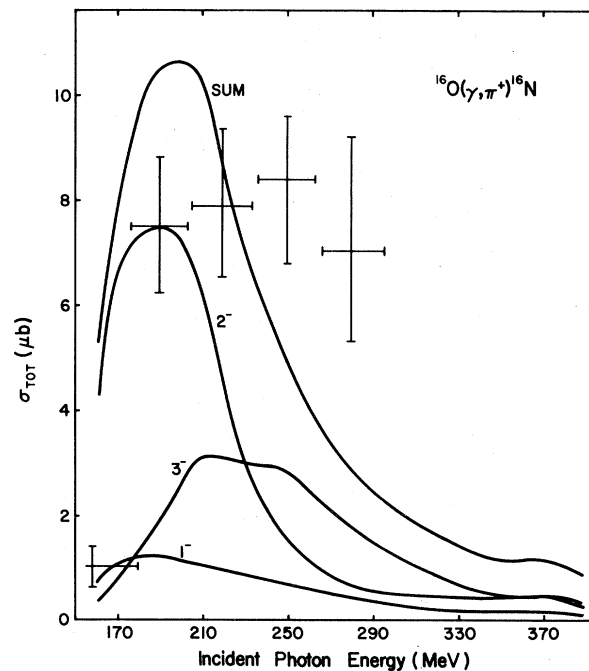


FIG. 8. Total cross sections for $^{16}\text{O}(\gamma, \pi^+)^{16}\text{N}$ to individual ^{16}N bound states and their sum (the 0^- contributions are too small to be seen on this scale). Data are from Meyer *et al.* (Ref. 5).

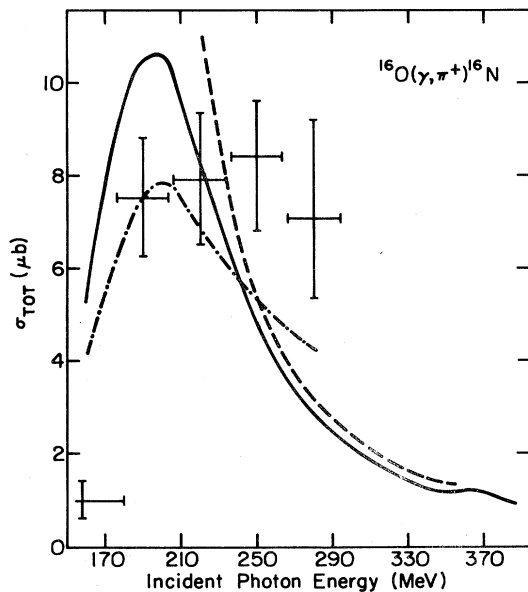


FIG. 9. Total cross sections for $^{16}\text{O}(\gamma, \pi^+)^{16}\text{N}$ for the sum of all four ^{16}N bound states. See Fig. 6 for theoretical curves. Data are from Meyer *et al.* (Ref. 5).

and uncertain subtractions for $^{17}\text{O}(\gamma, p)$ and $^{18}\text{O}(\gamma, pn)$ background contributions. We note in passing that a recent threshold measurement²⁵ led to a cross section of $8 \mu\text{b}$ at 160 MeV as compared to $1 \mu\text{b}$ for the Meyer experiment.

We have found that for both $A=10$ and $A=16$ the differences among parametrizations of elementary production amplitudes, nuclear wave functions, and pion optical potentials are not usually sufficient to cause major divergences in calculated results. At the same time, it is clear that much remains to be done in achieving quantitative agreement with experiment. It would be helpful if the differential cross section measurements for $A=16$ could be extended to lower energies and if the total cross section measurements could be carefully reexamined.

We are happy to acknowledge conversations and/or correspondence with A. M. Bernstein, K. I. Blomqvist, P. Bosted, V. Devanathan, M. Singham, and E. J. Winhold. We are grateful to W. Teeters for providing us with the Cohen-Kurath wave functions.

*Present address: Physics Department, DePauw University, Greencastle, Indiana 46135.

¹D. Rowley *et al.*, report, 1981 (unpublished).

²D. Rowley, Ph.D. thesis, Rensselaer Polytechnic Institute, 1981; E. J. Winhold (private communication).

³P. E. Bosted, K. I. Blomqvist, A. M. Bernstein, S. A. Dytman, and R. A. Miskimen, *Phys. Rev. Lett.* **45**, 1544 (1980).

⁴P. E. Bosted, Ph.D. thesis, MIT, 1980 (unpublished); and (private communication).

⁵R. A. Meyer, W. B. Walters, and J. P. Hummel, *Phys. Rev. B* **138**, 1421 (1965).

⁶M. Singham and F. Tabakin, quoted in Ref. 3; and (private communication).

⁷A. Nagl and H. Überall, quoted in Ref. 1; R. D. Graves *et al.*, *Can. J. Phys.* **58**, 48 (1980).

⁸V. Devanathan, V. Giriya, and G. N. Prasad, *Can. J. Phys.* **58**, 1151 (1980); V. Devanathan (private communication).

⁹I. Blomqvist and J. M. Laget, *Nucl. Phys.* **A280**, 405 (1977).

¹⁰S. Cohen and D. Kurath, *Nucl. Phys.* **73**, 1 (1965); W. Teeters (private communication).

¹¹K. Stricker, H. McManus, and J. A. Carr, *Phys. Rev. C* **19**, 929 (1979).

¹²F. A. Behrends, A. Donnachie, and D. L. Weaver, *Nucl. Phys.* **B4**, 54 (1967); 103 (1967).

¹³G. F. Chew, M. L. Goldberger, F. E. Low, and Y. Nambu, *Phys. Rev.* **106**, 1345 (1957).

¹⁴M. Rho, *Phys. Rev. Lett.* **18**, 671 (1967).

¹⁵N. Freed and P. Ostrander, *Phys. Lett.* **61B**, 449 (1976); I. Blomqvist *et al.*, *Phys. Rev. C* **15**, 988 (1977).

¹⁶E. J. Ansaldò, J. C. Bergstrom, R. Yen, and H. S. Caplan, *Nucl. Phys.* **A322**, 237 (1979).

¹⁷J. C. Bergstrom, *Phys. Rev. C* **21**, 2496 (1980).

¹⁸I. Sick, E. B. Hughes, T. W. Donnelly, J. D. Walecka, and G. E. Walker, *Phys. Rev. Lett.* **23**, 1117 (1969); T. W. Donnelly and G. E. Walker, *Ann. Phys. (N.Y.)* **60**, 209 (1970); T. W. Donnelly and J. D. Walecka, *Phys. Lett.* **41B**, 275 (1972); T. W. Donnelly and J. D. Walecka, *Annu. Rev. Nucl. Sci.* **25**, 329 (1975).

¹⁹The authors of Ref. 18 also carried out calculations in which they allowed the individual amplitudes to vary by $\leq 10\%$ from the TDA or RPA values (apart from the overall reduction factor) in order to obtain better agreement with weak and electromagnetic rates. We repeated our calculations with these perturbed wave functions but did not find qualitative differences with the results of the straight reduction factor calculations which are presented here.

²⁰C. W. DeJager, H. DeVries, and C. DeVries, *At. Data Nucl. Data Tables* **14**, 479 (1974).

²¹K. Stricker, J. A. Carr, and H. McManus, *Phys. Rev. C* **22**, 2043 (1980).

²²S. Maleki, Ph.D. thesis, Rensselaer Polytechnic Institute, 1981 (unpublished).

²³H. K. Lee and H. McManus, Nucl. Phys. A167, 257 (1971).

²⁴V. DeCarlo *et al.*, Phys. Rev. C 21, 1460 (1980).

²⁵E. C. Booth, B. Chasan, F. L. Milder, B. L. Roberts, and J. Comuzzi, Phys. Rev. C 20, 1603 (1979).